BASIC RESEARCH www.jasn.org

Autophagy Protects the Proximal Tubule from Degeneration and Acute Ischemic Injury

Tomonori Kimura,* Yoshitsugu Takabatake,* Atsushi Takahashi,* Jun-ya Kaimori,† Isao Matsui,* Tomoko Namba,* Harumi Kitamura,* Fumio Niimura,‡ Taiji Matsusaka,§ Tomoyoshi Soga,‖ Hiromi Rakugi,* and Yoshitaka Isaka*

*Department of Geriatric Medicine and Nephrology, Osaka University Graduate School of Medicine, Suita, Osaka, Japan; †Department of Advanced Technology for Transplantation, Osaka University Graduate School of Medicine, Suita, Osaka, Japan; ‡Department of Pediatrics, Tokai University School of Medicine, Isehara, Kanagawa, Japan; §Institute of Medical Science, Tokai University School of Medicine, Isehara, Kanagawa, Japan; and ‖Institute for Advanced Biosciences, Keio University, Kakuganji, Tsuruoka, Yamagata, Japan

ABSTRACT

Autophagy is a bulk protein degradation system that likely plays an important role in normal proximal tubule function and recovery from acute ischemic kidney injury. Using conditional *Atg5* gene deletion to eliminate autophagy in the proximal tubule, we determined whether autophagy prevents accumulation of damaged proteins and organelles with aging and ischemic renal injury. Autophagy-deficient cells accumulated deformed mitochondria and cytoplasmic inclusions, leading to cellular hypertrophy and eventual degeneration not observed in wildtype controls. In autophagy-deficient mice, I/R injury increased proximal tubule cell apoptosis with accumulation of p62 and ubiquitin positive cytoplasmic inclusions. Compared with control animals, autophagy-deficient mice exhibited significantly greater elevations in serum urea nitrogen and creatinine. These data suggest that autophagy maintains proximal tubule cell homeostasis and protects against ischemic injury. Enhancing autophagy may provide a novel therapeutic approach to minimize acute kidney injury and slow CKD progression.

J Am Soc Nephrol 22: 902–913, 2011. doi: 10.1681/ASN.2010070705

Macroautophagy (hereafter referred to as autophagy) is a highly conserved bulk protein degradation pathway in eukaryotes.[1,2] In the initial step of this process, parts of the cytoplasm and cellular organelles are engulfed within a double membrane vesicle called an autophagosome. This autophagosome fuses with lysosomes, resulting in the degradation of the sequestered materials by various lysosomal hydrolytic enzymes. Degradation is followed by the generation of amino acids that are recycled for macromolecular synthesis and energy production. Autophagy that occurs at low basal levels performs cellular homeostatic functions such as protein and organelle turnover.[1,2] Autophagy is upregulated when cells are preparing to undergo structural remodeling such as during developmental transitions or when cells wish to rid themselves of damaging cytoplasmic components.[3,4] This latter step is called autophagic flux.

Thus, autophagy not only plays the principal role in the supply of nutrients for cell survival but also plays a constitutive role in cellular homeostasis. Emerging evidence emphasizes the impor-

Received July 6, 2010. Accepted December 29, 2010.

Published online ahead of print. Publication date available at www.jasn.org.

Correspondence: Dr. Yoshitaka Isaka, Department of Geriatric Medicine and Nephrology, Osaka University Graduate School of Medicine, Box B6, 2-2 Yamada-oka, Suita, Osaka 585-0871, Japan. Phone: 81-6-6879-3857; Fax: 81-6-6879-3857; E-mail: isaka@kid.med.osaka-u.ac.jp

T. K. and Y.T. contributed equally to this work.

tance of autophagy in various biologic and pathologic processes. Recent genetic studies using tissue-specific autophagy-deficient mice have highlighted the importance of a basal level of autophagy in hepatocytes and neurons[5–7] and of both a basal level of autophagy and of autophagic flux in cardiomyocytes.[8,9]

Kidney demands high blood flow in relation to its weight, and this bulk supply is directed to the cortex,[10] where the proximal tubules consume a large amount of energy in the process of electrolyte reabsorption.[11] These tubules contain large quantities of mitochondria, which provide the energy for this reabsorption. Proximal tubules also contain large quantities of endoplasmic reticulum and ribosomes. The lysosomal system plays an important role in the reabsorption and degradation of albumin and low-molecular-weight plasma proteins from the glomerular filtrate.[12,13] Because proximal tubules are potentially energy wasting and work to degrade proteins, autophagy may play an important role in the physiology of proximal tubules. Moreover, kidney proximal tubules are susceptible to many kinds of insults such as ischemia-reperfusion (I/R) injury and nephrotoxic substrates. An important role of autophagy in proximal tubules is, therefore, suggested. The role of autophagy in kidney tubules has been shown in recent studies (normal and transplanted human kidney, cystinoic cells, and *in vitro* and *in vivo* models using autophagy inhibitors).[14–19] These studies suggested possible roles of autophagy in kidney tubules; however, to assess the role of autophagy directly, analysis of tissue-specific autophagy-deficient mice is necessary.[20,21]

In this study, we analyzed the role of autophagy in the kidney proximal tubules using proximal tubule-specific autophagy-deficient mice.

RESULTS

Ablation of the *Atg5* Gene in Proximal Tubular Epithelial Cells

To determine the basal function of autophagy in adult mouse proximal tubules of kidneys, we generated kidney proximal tubule-specific *Atg5*-deficient mice. We first generated a transgenic mouse that expresses Cre recombinase under the control of the promoter of the kidney androgen-regulated protein (*KAP*) gene (Supplementary Figure 1A). The *KAP* gene is normally expressed in the mouse fetal kidney during late pregnancy, and Cre expression is considered to occur during the development of kidney before birth.[22] The *KAP-Cre*/*CAG-CAT-Z* male mice showed LacZ-positive tubules in the cortex and the outer medulla (Supplementary Figure 1, C and D), whereas LacZ-positive tubules were absent in female mice (Supplementary Figure 1B). LacZ-positive tubules of both the outer stripe (Supplementary Figure 1E) and the medullary ray of the cortex (Supplementary Figure 1F) possessed a periodic acid-Schiff (PAS)-positive tall brush border, which is a characteristic trait of proximal tubules. Specific expression of Cre recombinase in the proximal tubule was thereby confirmed.

We crossed mice bearing an $Atg5^{flox}$ allele[5] with *KAP-Cre* transgenic mice. The resulting $Atg5^{flox/flox}$; $KAP\text{-}Cre^{+}$ male mice were indistinguishable in appearance from age-matched control $Atg5^{flox/flox}$; $KAP\text{-}Cre^{-}$ littermates. Western blot analysis showed efficient knockdown of the Atg5 protein in $Atg5^{flox/flox}$; $KAP\text{-}Cre^{+}$ mice (84.2 and 87.3% reduction in kidney cortex homogenates of 8-week-old mice and in isolated kidney proximal tubular cells of 3-week-old mice, respectively; Figure 1, A and B; Supplementary Figure 2). Consequently, conversion of microtubule-associated protein 1 light chain 3 (LC3)-I to LC3-II (a phosphatidylethanolamine conjugate)[23,24] was suppressed, and p62/sequestosome[25] accumulated in kidney cortex homogenates of 8-week-old mice and in isolated kidney proximal tubular cells of 3-week-old mice (Figure 1, A and B; Supplementary Figure 2).

Biologic Parameters in Proximal Tubule-Specific Autophagy-Deficient Mice

We first examined kidney function in the proximal tubule-specific autophagy-deficient mice. The kidney-to-body weight ratio was slightly increased in 8-week-old $Atg5^{flox/flox}$; $KAP\text{-}Cre^{+}$ mice compared with control littermates (Supplementary Table 1). All $Atg5^{flox/flox}$; $KAP\text{-}Cre^{+}$ mice and their littermates survived during the observational period (up to 9 months), and we observed no deterioration of kidney function as assessed by serum urea nitrogen and no increase in urinary albumin excretion in $Atg5^{flox/flox}$; $KAP\text{-}Cre^{+}$ mice compared with the littermates (8 weeks old; Supplementary Table 1; 9 months old; Supplementary Table 2).

$Atg5^{flox/flox}$; $KAP\text{-}Cre^{+}$ mice developed mild glycosuria at the age of 6 months compared with control littermates, whereas phosphaturia was not eminent (Figure 1C; Supplementary Figure 2C). Urinary amino acid analysis of 6-month-old $Atg5^{flox/flox}$; $KAP\text{-}Cre^{+}$ mice showed increased excretion of most of amino acids, with significant increase of excretion in threonine, tryptophan, valine, and alanine ($P < 0.05$; Figure 1D).

Histologic Changes in Proximal Tubule-Specific Autophagy-Deficient Mice

We then examined histologic changes in the autophagy-deficient kidney (Figure 2). Proximal tubule-specific autophagy-deficient mice showed few tubular changes at 3 weeks, but exhibited slight hypertrophy of the tubular cells without interstitial nephritis or fibrosis at 8 weeks (Figure 2A). Immunostaining of megalin, a marker of the proximal tubular brush border, showed that the hypertrophied cells are proximal tubular cells (Figure 2B). Accumulation of cytosolic amorphous substrates became apparent at 6 months (Figure 2A), and megalin-positive proximal tubular cells were filled with amorphous substrates at 9 months (Figure 2B). In addition, electron microscopic analysis of 8-week-old proximal tubule-specific

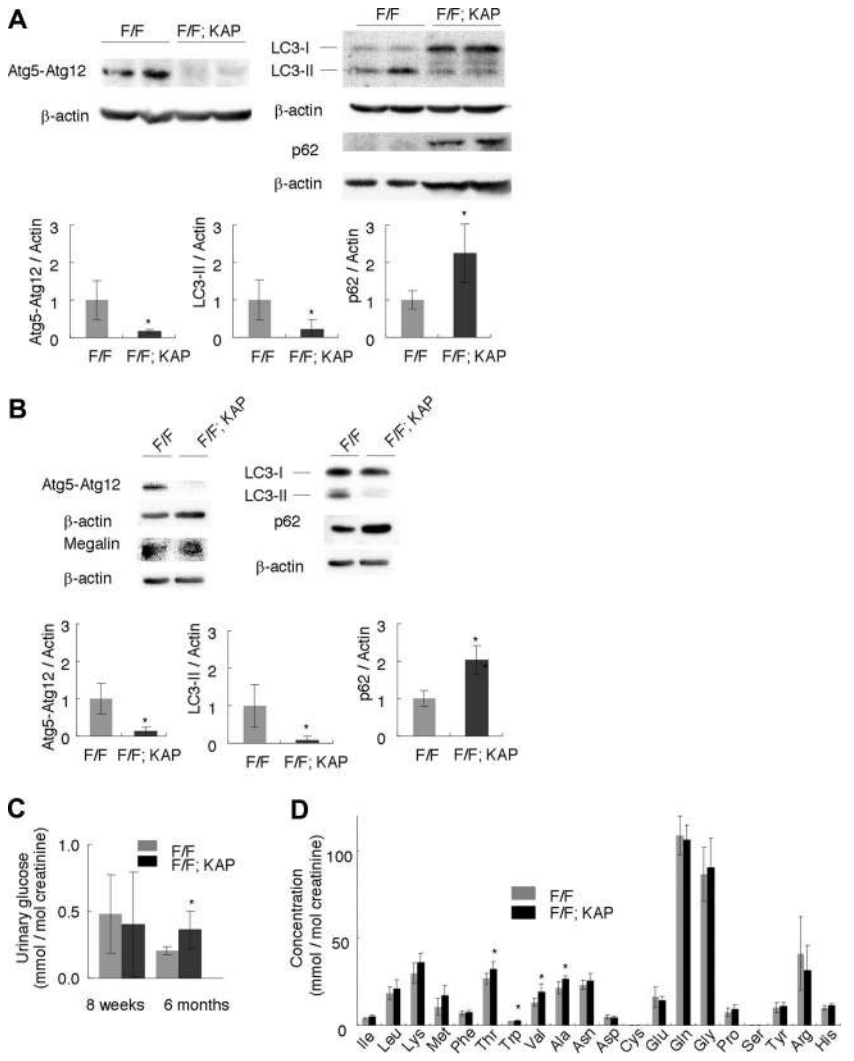

Figure 1. Physiologic changes in proximal tubule-specific autophagy-deficient mice. (A and B) Western blot analysis confirmed *Atg5* deficiency, suppression of the conversion of LC3-I to LC3-II, and accumulation of p62 in (A) kidney cortexes of 8-week-old *Atg5*$^{flox/flox}$; *KAP-Cre*$^{+}$ (F/F; KAP) mice ($n = 5$) and in (B) lysates of isolated proximal tubular cells of 3-week-old *Atg5*$^{flox/flox}$; *KAP-Cre*$^{+}$ mice ($n = 3$ to 4). A representative immunoblot is shown. The graph shows the ratios of band intensities of Atg5-Atg12, LC3-II, and p62 to those of actin, standardized to the mean of the control. Megalin was blotted as a marker of the proximal tubular cells. (C) Glycosiuria was observed in 6-month-old *Atg5*$^{flox/flox}$; *KAP-Cre*$^{+}$ mice ($n = 5$ to 6). (D) Mild amino aciduria was observed in 6-month-old *Atg5*$^{flox/flox}$; *KAP-Cre*$^{+}$ mice ($n = 5$ to 6). Cysteine and serine were not detected. Data are presented as means ± SD. *$P < 0.05$ *versus* *Atg5*$^{flox/flox}$; *KAP-Cre*$^{-}$ mice of same age.

autophagy-deficient mice showed accumulation of numerous crescent membranous structures in the tubular epithelial cells, mainly adjacent to the mitochondria (Figure 2, C and D). Numerous creascent membranous structures were also seen in 9-month-old proximal tubule-specific autophagy-deficient mice, although their sizes were smaller (Figure 2, E and F). Of note, accumulation of deformed mitochondria was exclusively observed in autophagy-deficient mice (Figure 2G). Because deficiency in basal autophagy has been reported to induce the accumulation of protein aggregations in other organs,[5–7] we stained a kidney specimen from the *Atg5*$^{flox/flox}$; *KAP-Cre*$^{+}$ mice with anti-p62 and anti-ubiquitin antibodies. The p62 protein is known to be selectively degraded by autophagy, and ubiquitin is known to accumulate within aggregates. Massive accumulation of p62- and ubiquitin-positive inclusions were observed in 9-month-old *Atg5*$^{flox/flox}$; *KAP-Cre*$^{+}$ mice, whereas they were rarely seen in younger *Atg5*$^{flox/flox}$; *KAP-Cre*$^{+}$ mice (Figure 3A). Immunofluorescence analysis showed that p62- and ubiquitin-positive inclusions were almost exclusively seen in the proximal tubules of 9-month-old *Atg5*$^{flox/flox}$; *KAP-Cre*$^{+}$ mice (Figure 3, B and C) and that p62 and ubiquitin co-localized in these inclusion bodies (Figure 3D).

Effect of Autophagy Deficiency under Pathologic Conditions

We analyzed the role of autophagy in kidney pathophysiology using a kidney I/R injury model. We first examined the induction of autophagy after I/R injury using green fluorescence protein (GFP)-LC3 transgenic mice.[24] I/R injury induced significant increase in the number of LC3 dots in a time-dependent manner, with its peak of 24 hours after I/R injury, whereas GFP-LC3 dots were rarely seen in sham-operated mice (Figure 4A; Supplementary Figure 3). GFP-LC3 dots were mainly localized in damaged proximal tubules as assessed by co-immunostaining with *Lotus tetragonolobus* lectin, a marker of proximal tubules (Figure 4A). Increased GFP-LC3 dots were accompanied by elevated cytoplasmic and nuclear LC3 signals (significance of nuclear LC3 signals is unknown[21]; Figure 4A). LC3 also co-localized with p62 and ubiquitin (Figure 4, B and C).

We next exposed the *Atg5*$^{flox/flox}$; *KAP-Cre*$^{+}$ mice to I/R injury. Western blot analysis showed that the conversion of LC3-I to LC3-II was suppressed in the kidney cortexes of *Atg5*$^{flox/flox}$; *KAP-Cre*$^{+}$ mice compared with the corresponding controls after I/R injury (Supplementary Figure 4), indicating that autophagy was suppressed in *Atg5*$^{flox/flox}$; *KAP-Cre*$^{+}$ mice under this condition. We observed severely injured tubules with massive tubular sediments and vacuolation in the kidney cortex of I/R-injured *Atg5*$^{flox/flox}$; *KAP-Cre*$^{+}$ mice in comparison to I/R-injured control littermates (Figure 5A). The tubular injury score of the *Atg5*$^{flox/flox}$; *KAP-Cre*$^{+}$ mice was significantly in-

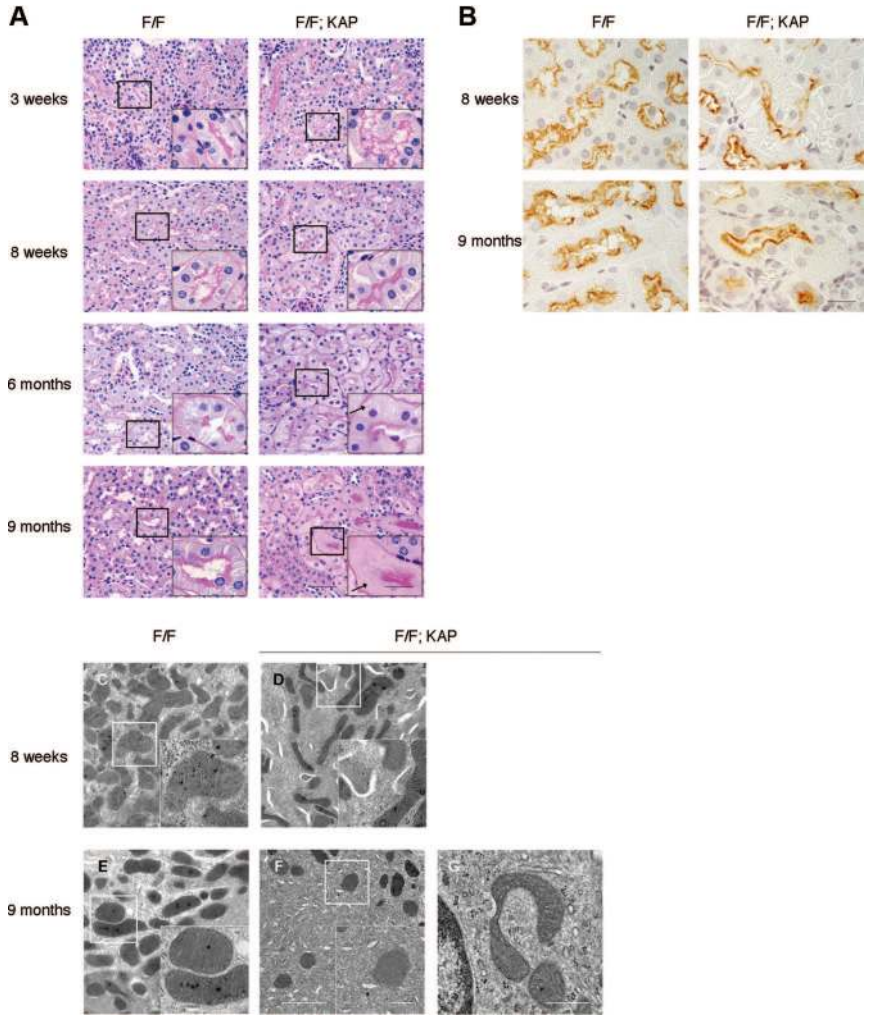

Figure 2. Histologic changes in proximal tubule-specific autophagy-deficient mice. (A) PAS-stained kidney cortex from 3-week-old, 8-week-old, 6-month-old, and 9-month-old*Atg5*$^{flox/flox}$; *KAP-Cre*$^{-}$ (left) and *Atg5*$^{flox/flox}$; *KAP-Cre*$^{+}$ (right) mice ($n = 4$ to 5). *Atg5*$^{flox/flox}$; *KAP-Cre*$^{+}$ mice exhibited slight hypertrophy of the tubular cells at 8 weeks and accumulation of cytosolic amorphous substrates at 6 months. Arrows indicate tubular cells with cytosolic accumulation of amorphous substrates. Bars, 50 and 20 μm (insets). (B) Immunostaining of megalin, a marker of the proximal tubular brush border, showed that the hypertrophied cells (8 weeks) and amorphous substrates-accumulated cells (9 months) are proximal tubular cells in *Atg5*$^{flox/flox}$; *KAP-Cre*$^{+}$ mice ($n = 5$). Bar, 20 μm. (C–E) *Atg5* deficiency causes accumulation of crescent-like structures and deformed mitochondria. Electron micrographs of kidney proximal tubules from *Atg5*$^{flox/flox}$; *KAP-Cre*$^{-}$ (C and E) and *Atg5*$^{flox/flox}$; *KAP-Cre*$^{+}$ (D, F, and G) mice of 8 weeks (C and D) and 9 months (E through G) of age. The autophagy-deficient proximal tubular cells showed accumulation of crescent-like structures in 8-week-old (D) and 9-month-old (F) mice. (G) The autophagy-deficient proximal tubular cells of 9-month-old mice also contained deformed mitochondria. The figure is a representative of multiple experiments ($n = 3$). Bars, 2 μm (C–F) and 500 nm (insets of C–F and G). Magnification, ×400 (A), ×1000 (insets of A and B), ×2500 (C through F), and ×10,000 (insets of C–F and G).

creased compared with that of controls (Figure 5A). Bilateral I/R injury caused significant increase of serum urea nitrogen and creatinine in *Atg5*$^{flox/flox}$; *KAP-Cre*$^{+}$ mice compared with I/R-injured control littermates (Figure 5B). The number of apoptotic, Terminal deoxynucleotidyl transferase-mediated deoxyuridine triphosphate nick end-labeling-positive tubular cells increased in *Atg5*$^{flox/flox}$; *KAP-Cre*$^{+}$ mice after I/R injury (Figure 5C).

Immunohistologic analysis indicated a massive accumulation of ubiquitin-positive and p62-positive large dots in the kidney tubular cells of *Atg5*$^{flox/flox}$; *KAP-Cre*$^{+}$ mice after I/R injury compared with sham-operated *Atg5*$^{flox/flox}$; *KAP-Cre*$^{+}$ mice or of I/R-injured *Atg5*$^{flox/flox}$; *KAP-Cre*$^{-}$ mice (Figure 6). Immunofluorescence analysis confirmed that these p62- and ubiquitin-positive large dots were co-localized in the megalin-labeled proximal tubular cells (Figure 7, A–C). These dots were not seen in other part of the tubules (distal tubules [Supplementary Figure 5A] or thick ascending limb of the loop of Henle [Supplementary Figure 5B]). Collectively, these results suggest there were massive accumulations of inclusions that contain both ubiquitin and p62 after I/R injury in autophagy-deficient kidney proximal tubules.

DISCUSSION

This study showed that autophagy has an essential role in proximal tubular homeostatic control both physiologically and pathophysiologically. Proximal tubule-specific autophagy-deficient mice exhibited gradual and massive accumulation of amorphous substrate and p62- and ubiquitin-inclusions in the cytosol, thereby resulting in hypertrophy of kidney proximal tubules. I/R injury increased autophagic flux as assessed by massive accumulation of LC3 dots in GFP-LC3 transgenic mice. The proximal tubule-specific autophagy-deficient mice exhibited remarkably more severe injury than controls with rapid accumulation of p62- and ubiquitin-positive inclusions in the proximal tubules in response to I/R injury, showing that autophagy plays a protective role against I/R injury. These observations proved our hypothesis that basal autophagy regulates tubular homeostasis against aging stress under physiologic conditions and that autophagic flux protects tubules under pathologic conditions (shown in Supplementary Figure 6).

The role of autophagy in tubular cells has been studied in *in*

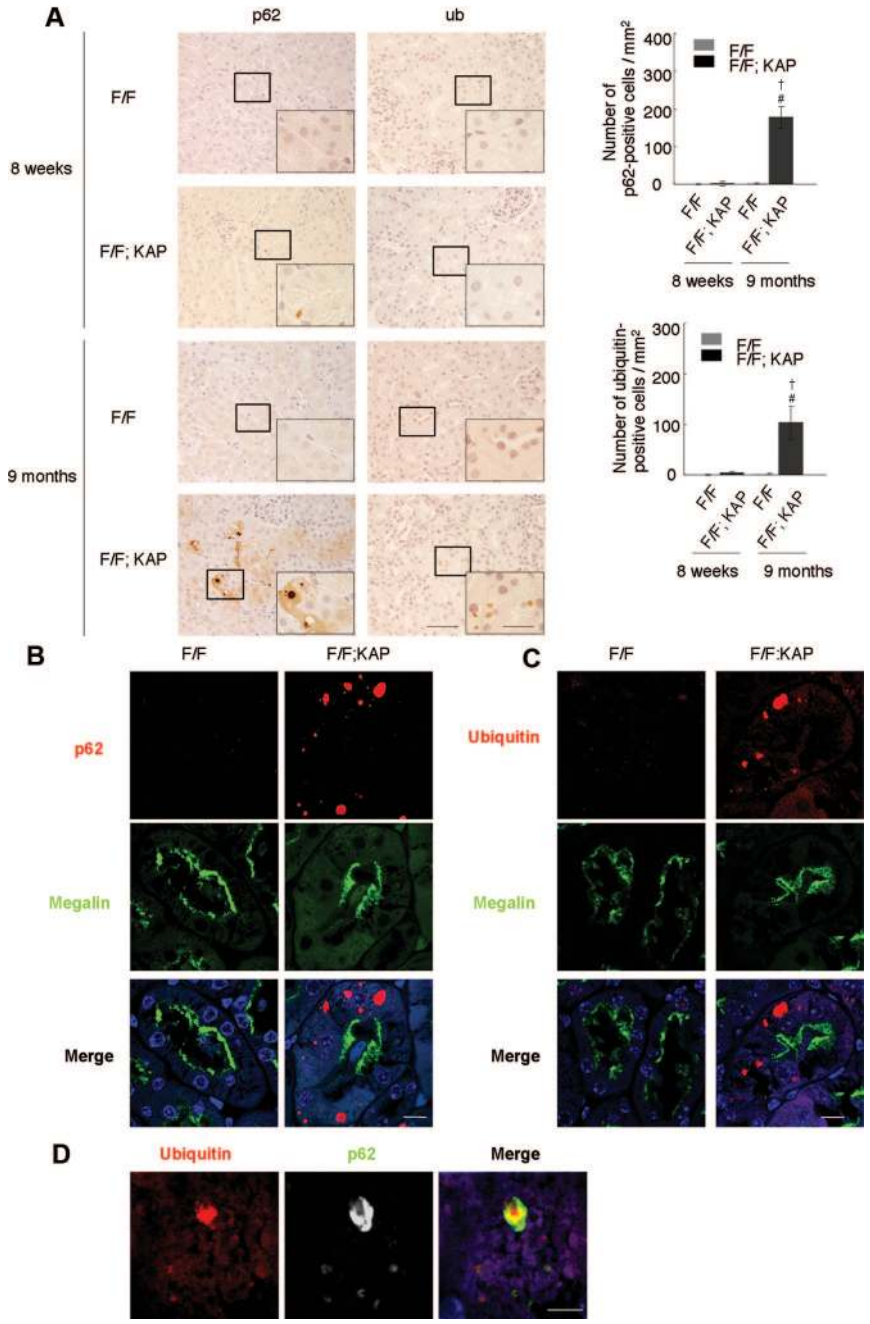

Figure 3. *Atg5* deficiency causes accumulation of p62- and ubiquitin-positive inclusions in the kidney cortex tubular cells of 9-month-old mice. (A) Immunohistologic analysis of *Atg5*$^{flox/flox}$; *KAP-Cre*$^{-}$ and *Atg5*$^{flox/flox}$; *KAP-Cre*$^{+}$ mice kidney cortexes from 8-week-old and 9-month-old mice. Kidney tubular cells of 8-week-old mice showed little staining of p62 (left) or ubiquitin (right), whereas those of 9-month-old mice showed massive accumulation of p62- and ubiquitin -positive inclusions in *Atg5*$^{flox/flox}$; *KAP-Cre*$^{+}$ mice. These inclusions were not obsereved in *Atg5*$^{flox/flox}$; *KAP-Cre*$^{-}$ mice. $^{\dagger}P < 0.05$ *versus* 8-week-old *Atg5*$^{flox/flox}$; *KAP-Cre*$^{+}$ mice; $^{\#}P < 0.05$ *versus* 9-month-old *Atg5*$^{flox/flox}$; *KAP-Cre*$^{-}$ mice. Data are presented as means ± SD. (B and C) Immunofluorescence analysis showed that marked accumulation of p62-positive (B) and ubiquitin-positive (C) large dots was observed in autophagy-deficient kidney proximal tubules of 9-month-old mice. Megalin was used as a marker of the proximal tubules. DAPI staining was performed as a counterstaining. (D) p62 and ubiquitin colocalized in the inclusions of autophagy-deficient kidney proximal tubules of 9-month-old mice. The figure is representative of a multiple experiments ($n = 5$). Bars, 50 (A), 20 (insets of A), 10 (B and C), and 5μm (D). Magnification, ×400 (A), ×1000 (Inlets), ×352 (B and C), and ×1058 (D).

vitro and *in vivo* models.[15–17] These studies mainly used autophagy inhibitors (*e.g.*, 3-methyladenine) or gene knockdown to modulate the activity of autophagy. Autophagy inhibitors are known to inhibit not only autophagy but also inhibit many other degradative pathways (*e.g.*, proteasome, lysosomal function, mitochondrial function, or endocytosis).[20,21,26–28] The blockage of proteasome, for example, may activate autophagy, leading to unexpected results caused by the crosstalk among the degradative systems. Functional knockdown (*e.g.*, with RNAi) is sometimes difficult to block autophagy completely.[20,21,29] Therefore, gene deletion is the preferred approach to determine the precise role of autophagy both in physiologic and pathologic processes. Because systemic autophagy-deficient mice die during the early neonate period,[30] tissue-specific gene depletion has been conducted in several organs.[9,20,21] Here, we showed, for the first time, that the basal and flux level of autophagy plays a prerequisite role in proximal tubular cells using tissue-specific autophagy-deficient mice.

Thus far, the basal level of autophagy in proximal tubules has been underestimated based on the following observations of GFP-LC3 transgenic mice: (*1*) GFP-LC3–positive autophagosomes were rarely observed in steady state of tubular epithelial cells and (*2*) starvation induces only a slight increase in the number of GFP-LC3 dots in the tubules.[24] However, our data clearly showed that the basal level of autophagy plays a critical role in the homeostasis of proximal tubular cells using conditional autophagy-deficient mice.

First, it is noteworthy that defective autophagy resulted in the accumulation of deformed mitochondria in the kidney proximal tubules (Figure 2G). Similar observations have been reported in other tissue-specific autophagy-deficient cells, including liver and heart.[6,8] The proximal tubules mainly depend their energy supply on aerobic metabolism and are therefore

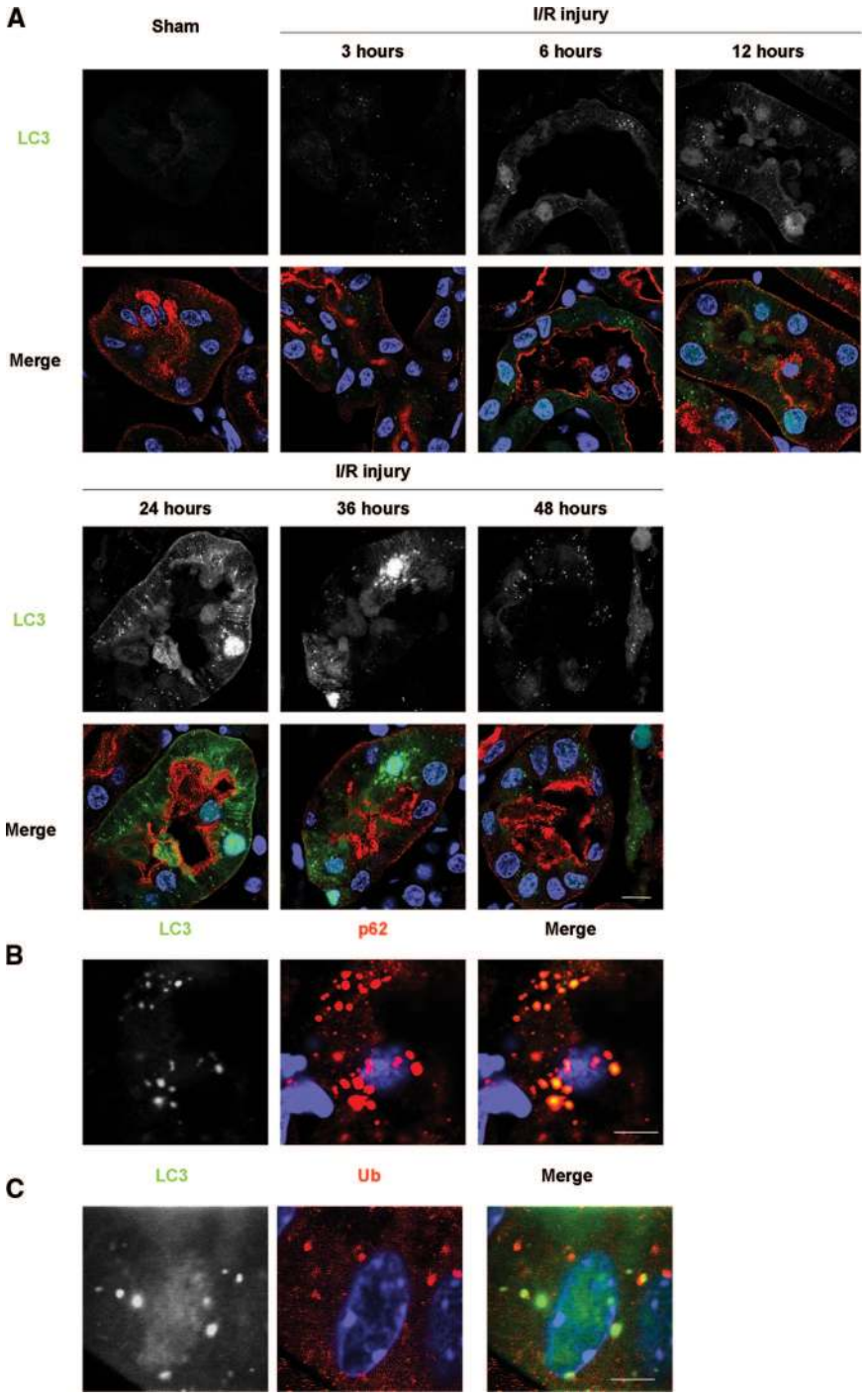

Figure 4. Formation of LC3 dots in kidney proximal tubules of LC3-GFP transgenic mice in response to I/R injury. (A) The presence of LC3-positive dots in the proximal tubules of the kidney of LC3-GFP transgenic mice was examined by immunofluorescence analysis after a sham operation and after 3, 6, 12, 24, 36, and 48 hours after unilateral I/R injury. The number of LC3 dots increased time-dependently after injury for up to 24 hours, after which it decreased. *Lotus tetragonolobus* lectin (LTA) was used as a marker of proximal tubules, and DAPI staining was performed as a counterstaining. (B and C) LC3 dots colocalized with p62 (B) and ubiquitin dots (C) after I/R injury. Kidney tissues 12 hours after unilateral I/R injury is shown. The figure is representative of a multiple experiments ($n = 3$ to 5). Bars, 10 (A) and 5 μm (B and C). Magnification, $\times$352 (A), $\times$1058 (B), and $\times$1408 (C).

extremely vulnerable to mitochondrial damages.[31] Damaged mitochondria generates intrinsic reactive oxygen species, which accelerates the aging process.[32,33] Recent studies suggested that clearance of damaged mitochondria is also an important role for autophagy (mitophagy)[34,35] and that autophagy may counteract the aging process through quality control of the mitochondria. Our findings strongly suggest that autophagy in kidney proximal tubules contributes to cellular homeostasis by eliminating damaged mitochondria, although the precise mechanism remains to be elucidated.

Second, electron microscopic analysis of autophagy-deficient kidneys also showed the accumulation of crescent membranous structures adjacent to the mitochondria in tubular epithelial cells. These structures were prominent in 8-week-old mice but obscured in 9-month-old mice, probably because of the mass effect of inclusions. Similar observations have been reported in starved *Atg5*-deficient ES cells.[36] We assume that these structures are intermediate structures formed during the disorganized autophagic process. It is of interest to consider why these structures are mainly observed adjacent to the mitochondria. The damaged mitochondria may produce a signal to initiate autophagy, resulting in their own degradation. Alternatively, autophagosomes can be formed from the outer membrane of mitochondria,[37] which is consistent with our observation that the large number of crescents exist along with the deformed mitochondria in autophagy-deficient tubular cell.

Third, old proximal tubular-specific autophagy-deficient mice exhibited proximal tubular dysfunction, *e.g.,* increased excretion of amino acid and glycosuria. These dysfunctions were not so prominent, probably because KAP is expressed mainly in restricted segments of proximal tubules, and the poximal tubular function may be compensated by the rest of the segments. We selected *ad libitum* because dietary restriction may induce autophagy; however, this method may have affected the results of urinary analyses.

Fourth, the proximal tubule-specific autophagy-deficient mice exhibited accumulation of p62- and ubiquitin-positive inclu-

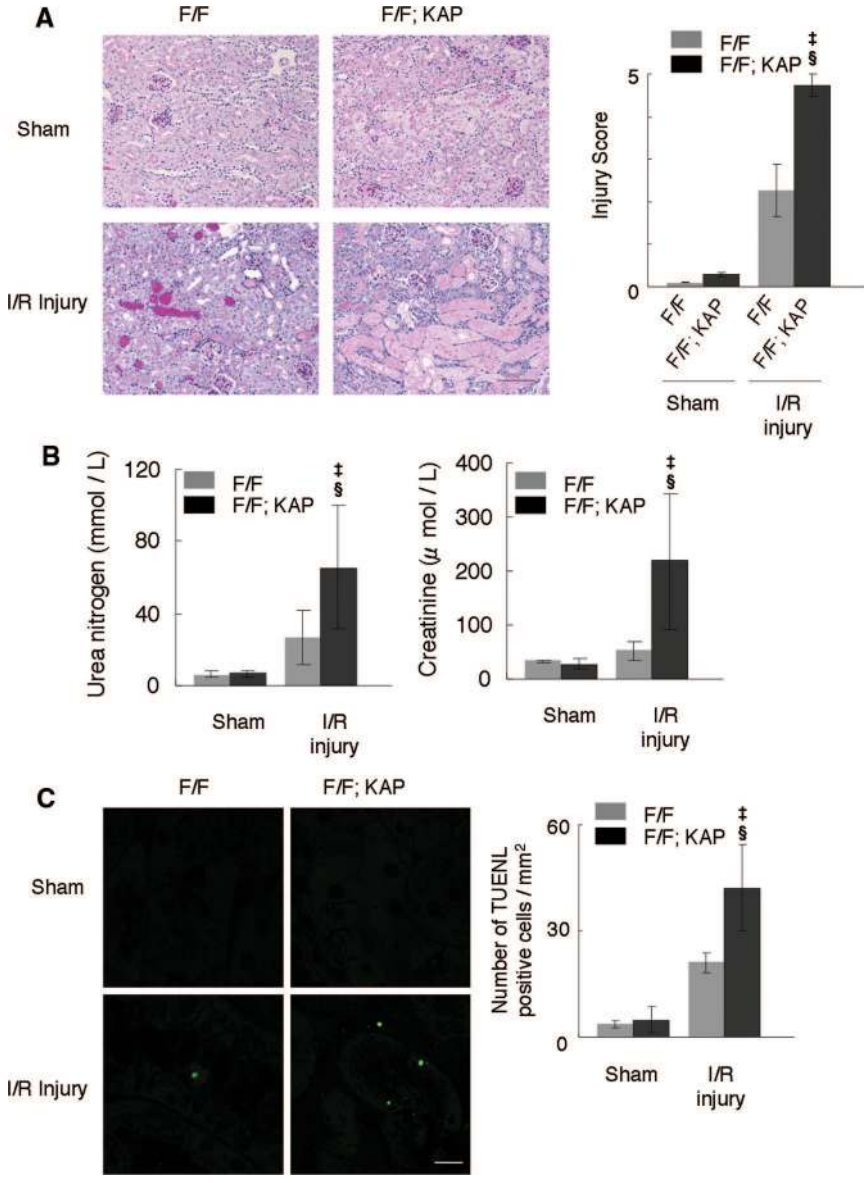

Figure 5. Marked injury in autophagy-deficient kidney cortex after I/R injury. (A) Histologic analysis of *Atg5*$^{flox/flox}$; *KAP-Cre*$^{-}$ (left) and *Atg5*$^{flox/flox}$; *KAP-Cre*$^{+}$ (right) kidneys 2 days after unilateral I/R injury ($n = 5$). PAS-stained kidney cortexes showed that the tubules of *Atg5*$^{flox/flox}$; *KAP-Cre*$^{+}$ mice were severely injured compared with I/R-injured *Atg5*$^{flox/flox}$ mice. The tubular injury score of the *Atg5*$^{flox/flox}$; *KAP-Cre*$^{+}$ mice was significantly increased compared with that of controls. (B) Bilateral I/R injury caused significant increase of serum urea nitrogen and creatinine in *Atg5*$^{flox/flox}$; *KAP-Cre*$^{+}$ mice compared with I/R-injured control littermates ($n = 4$ to 6). (C) Terminal deoxynucleotidyl transferase-mediated deoxyuridine triphosphate nick end-labeling staining 2 days after I/R injury showed increased number of apoptotic tubular cells in the cortex of *Atg5*$^{flox/flox}$; *KAP-Cre*$^{+}$ mice ($n = 5$). $^{‡}P < 0.05$ *versus* sham-operated *Atg5*$^{flox/flox}$; *KAP-Cre*$^{+}$ mice; $^{§}P < 0.05$ *versus* I/R injury-operated *Atg5*$^{flox/flox}$; *KAP-Cre*$^{-}$ mice. Data are presented as means ± SD. Bars: 100 (A) and 10 μm (C). The images are representatives of multiple experiments. Magnification, ×200 (A) and ×352 (C).

sion bodies in a time-dependent manner. Nine-month-old proximal tubule-specific autophagy-deficient mice showed a massive amount of inclusion bodies, whereas inclusion bodies were rarely seen in younger mice. Accumulation of inclusion bodies caused by a defect in the basal level of autophagy has been reported in neuron- and liver-specific knockout mice.[5–7] Neuron-specific knockout mice developed neurodegeneration with accumulation of cytoplasmic inclusion bodies and died earlier than controls.[5,7] Liver-specific knockout mice developed hepatomegaly and hepatic cell swelling with accumulation of inclusion bodies.[6] The precise role of inclusion bodies remain to be elucidated, but it is quite possible that aggregated proteins are known to cause cellular damage in several ways such as by increasing oxidative stress and endoplasmic reticulum stress and by triggering apoptosis.[38–40]

We used an I/R injury model of the kidney to determine the role of autophagic flux in proximal tubule cells because postischemic acute kidney injury is the most important cause of acute kidney injury, and proximal tubular cells are the main lesion of this injury.[41] For I/R injury, we used 8-week-old mice because we found only minor difference between *Atg5*$^{flox/flox}$; *KAP-Cre*$^{+}$ mice and *Atg5*$^{flox/flox}$ mice at the age of 8 weeks. We found that the proximal tubule-specific autophagy-deficient mice exhibited more severe injury than control mice, with rapid accumulation of p62- and ubiquitin-positive inclusion bodies in response to I/R injury, showing that autophagy plays a protective role against I/R injury.

The potential mechanisms of renoprotection by autophagy in the I/R injury model remains unknown. One possible mechanism is that autophagy may eliminate damaged mitochondria. I/R injury induces fragmentation of the mitochondria, which leads to mitochondrial outer membrane permeabilization, the release of apoptogenic factors, and consequent apoptosis.[42,43] Moreover, mitochondrial activity could cause excessive energy consumption and could also become a source of intrinsic ROS.[32,33] Therefore, it is possible that failure to clear damaged mitochondria caused by defective autophagy might lead to cell death under ischemic conditions.

Another possibility is that autophagy protects cells by avoiding accumulation of aggregate-prone proteins that is generated in response to I/R injury. In line with this discussion, the proximal tubule-specific autophagy-deficient kidney showed rapid accumulation of p62- and ubiqui-

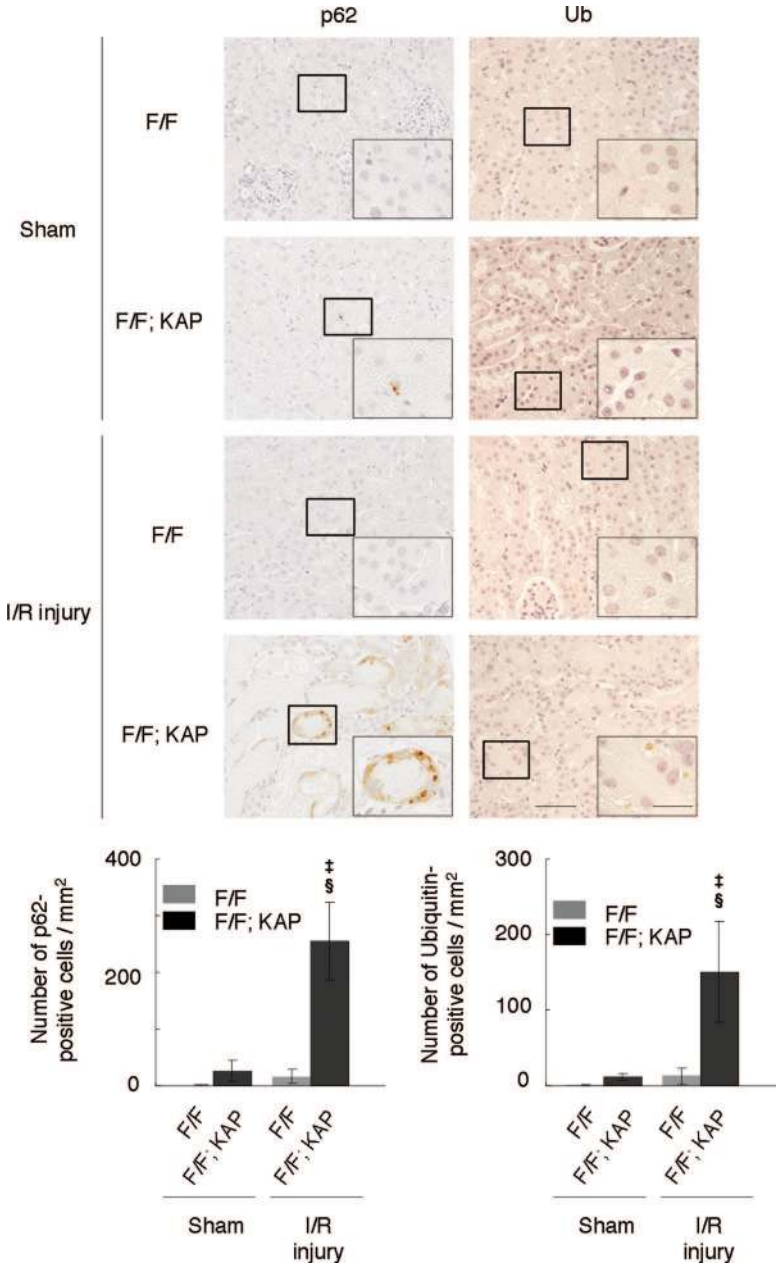

Figure 6. Accumulation of p62- and ubiquitin-positive inclusions in the autophagy-deficient kidney cortex after I/R injury. Immunohistologic analysis of *Atg5*$^{flox/flox}$; *KAP-Cre*$^{-}$ and *Atg5*$^{flox/flox}$; *KAP-Cre*$^{+}$ kidneys 2 days after I/R injury. p62 (left) or ubiquitin (right) staining of kidney cortexes showed massive accumulation of p62- and ubiquitin-positive inclusions in *Atg5*$^{flox/flox}$; *KAP-Cre*$^{+}$ kidneys after I/R injury. $^{\ddagger}P < 0.05$ *versus* sham-operated *Atg5*$^{flox/flox}$; *KAP-Cre*$^{+}$ mice; $^{\S}P < 0.05$ *versus* I/R injury-operated *Atg5*$^{flox/flox}$; *KAP-Cre*$^{-}$ mice. Data are presented as means ± SD. The figure is a representative of multiple experiments ($n = 5$). Bars, 50 and 20 μm (insets). Magnification, ×400 and ×1000 (insets).

tin-positive inclusion bodies. Degradation systems are functionally coupled, and it is quite possible that, during certain conditions, accumulation of ubiquitinated proteins might exceed capacity of proteasomal degradation, resulting in a buildup of ubiquitinated proteins and formation of protein aggregates.[44] Therefore, functional elevation of autophagic clearance activity by some reagent may provide the therapeutic tool for I/R injury of the kidney.

In conclusion, we showed that (*1*) a basal level of autophagy plays a critical role in kidney tubular homeostasis and (*2*) autophagic flux plays a protective role against disease of tubular epithelial cells under pathologic conditions. Further understanding of the process of autophagy of the kidney may provide a novel therapeutic approach to prevent chronic kidney disease and acute kidney injury.

CONCISE METHODS

Generation of KAP-Cre Transgenic Mice

A Cre cDNA fragment obtained from the pCre-Pac plasmid (Kurabo)[45] was combined with a 4.0-kb *KAP* promoter fragment and with the intron and poly (A)$^{+}$ of the rabbit β-globin gene (Supplementary Figure 1A). The resultant transgene was injected into the pronuclei of fertilized eggs, obtained from BDF1 × C57BL/6N mating, to generate *KAP-Cre* mice. The *KAP-Cre* mice were used after backcrossing with C57BL/6N more than nine times.

Animals

Mice bearing an *Atg5*^{flox} allele, in which exon 3 of the *Atg5* gene is flanked by two *loxP* sequences, have been described previously.[5] Genomic DNA isolated from mice bearing an *Atg5*^{flox} was subjected to PCR analysis. Progeny containing the *Atg5*^{flox} allele were bred with the *KAP-Cre* transgenic mice to generate *Atg5*$^{flox/flox}$; *KAP-Cre*$^{+}$ mice. GFP-LC3 transgenic mice have been described previously.[24] The mice were maintained individually and allowed access to water and mouse chow *ad libitum*. All animal experiments were approved by the institutional committee of the Animal Research Committee of Osaka University and in accordance with the Guidelines for Animal Experiments of Osaka University and the Japanese Animal Protection and Management Law (No. 25).

Histologic Analysis

Mice were transcardially perfused with 4% paraformaldehyde in phosphate buffer (pH 7.4). Tissues were postfixed and embedded in paraffin or frozen in optimum cutting temperature compound (Tissue Tek; Miles Laboratories). We performed PAS, hematoxylin and

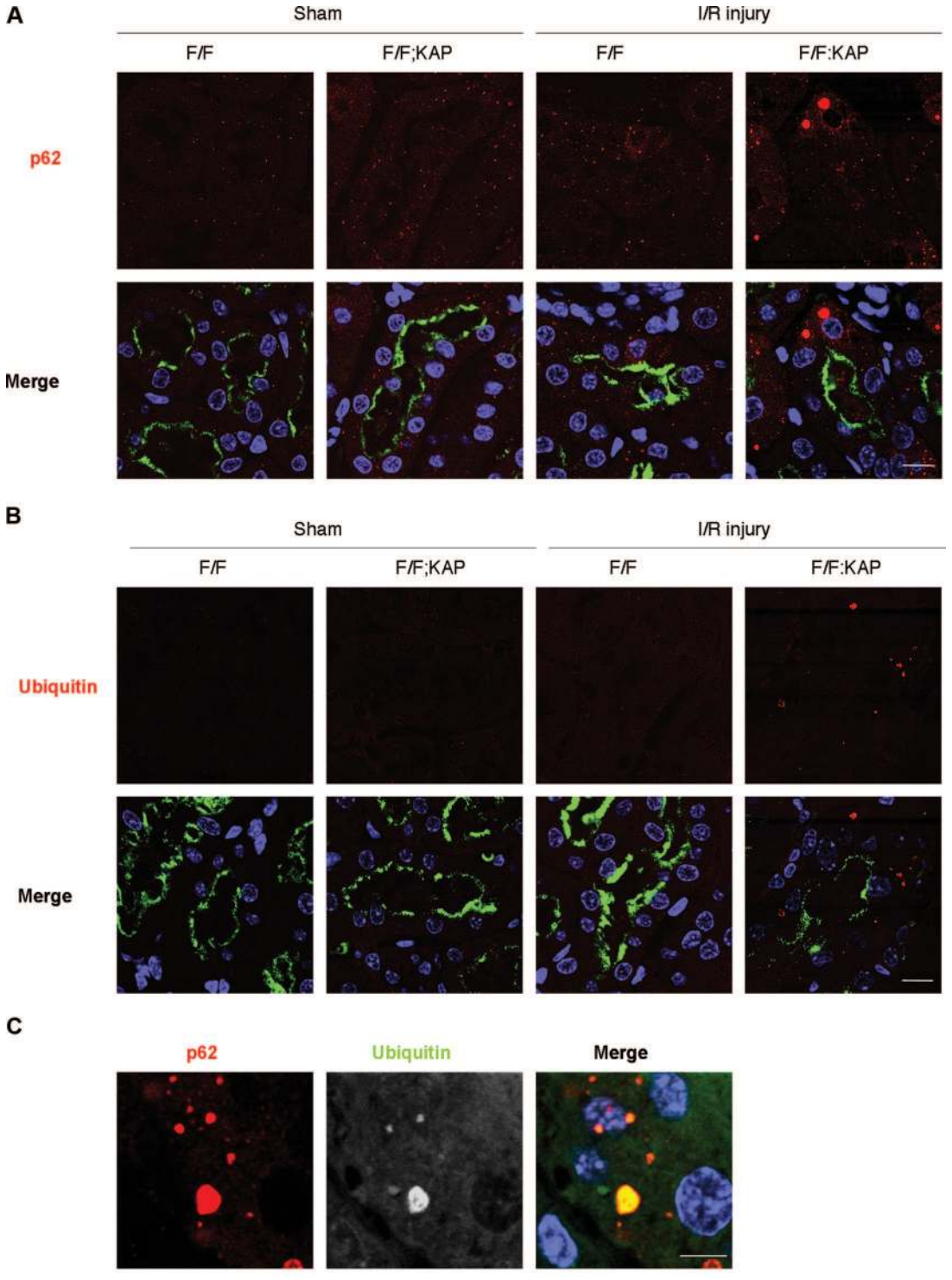

Figure 7. Formation of p62- and ubiquitin-positive inclusions in autophagy-deficient kidney proximal tubules in response to I/R injury. (A and B) Immunofluorescence analysis showed that marked accumulation of p62-positive large dots (A) and ubiquitin-positive dots (B) was observed in autophagy-deficient kidney proximal tubules 2 days after I/R injury. (C) p62 and ubiquitin colocalized in the inclusions of autophagy-deficient kidney proximal tubules 2 days after I/R injury. Megalin was stained as a marker of proximal tubules in A and B. The figure is a representative of multiple experiments ($n = 5$). Bars, 10 (A and B) and 5 μm (C). Magnification, $\times$352 (A and B) and $\times$1058 (C).

eosin, and Masson-Trichrome staining. Paraffin or frozen sections were immunolabeled, and the immunofluorescence images were collected using a Leica TCS SP5 (Leica Microsystems CMS, Mannheim, Germany). Apoptotic cells were detected by Terminal deoxynucleotidyl transferase-mediated deoxyuridine triphosphate nick end-labeling assay using an *in situ* apoptosis detection kit (Takara Bio, Tokyo,

Japan). For electron microscopy, the kidneys were fixed with 2.5% glutaraldehyde and observed using a Hitachi H-7650 transmission electron microscope (Hitachi, Tokyo, Japan).

X-gal Staining

CAG-CAT-Z mice (a gift from Jun-ichi Miyazaki) expressing LacZ after Cre-mediated recombination was described previously.[47] *CAG-CAT-Z* mice were bred with *KAP-Cre* transgenic mice to establish double transgenic heterozygote mice. After death, kidneys were dissected, embedded in optimum cutting temperature compound, and frozen. Four-micrometer sections were fixed in 2% glutal aldehyde for 10 minutes at 4°C and stained in X-gal solution (1 mg/ml X-gal, 5 mM potassium ferricyanide, and 5 mM potassium ferrocyanide in PBS) overnight at 37°C. The section was fixed again with 4% paraformadlehyde for 10 minutes at 4°C and subjected to PAS staining.

Kidney I/R Injury Induction

Kidney ischemia was induced in male mice of 8 weeks. In brief, the animals were anesthetized and were kept on a homeothermic table. For unilateral clamping, back incisions were made to expose the kidney pedicles to induce 40 minutes of kidney ischemia. For bilateral clamping, front incisions were made, and 35 minutes of ischemia was introduced to the kidneys. The clamps were released for reperfusion for the indicated times. Control animals were subjected to sham operation without renal pedicle clamping. Kidney tubular cells of the cortex were examined by two nephrologists in a blind manner and were scored according to the percentage of damaged tubules: 0, no damage; 1, <25% damage; 2, 25 to 50% damage; 3, 50 to 75% damage, 4, 75 to 90% damage; and 5, >90% damage. Tubular damage was defined as cell necrosis, which was evaluated in this study by loss of brush border, tubular dilation, and cast formation. At least 15 to 20 fields (×400) were reviewed for each PAS-stained slide.

Isolation and Characterization of Mouse Kidney Proximal Tubule Cells

We isolated kidney proximal tubule cells from 3-week-old male mice as described below. After anesthetization, the kidneys were immediately removed and placed in cold (4°C) phosphate buffer. The renal capsule was removed, and the kidney was sagittally cut into two halves. The medulla was dissected and discarded from each half. The remaining cortical tissue was minced and transferred to 10 ml HBSS containing Collagenase Type II (Life Technologies, Grand Island, NY; 200 units/ml) and hyaluronidase (Wako Pure Chemical Industries, Osaka, Japan; 0.2%). Tubules were incubated at 37°C while rotating for 2 hours. After digestion, the tubule suspension was centrifuged at 150 × *g*. Selection of proximal tubules was performed using the CELLection Biotin Binder Kit (Invitrogen, Carlsbad, CA) according to the manufacturer's instructions and the biotinylated *Lotus tetragonolobus* agglutinin lectin (Vector Laboratories, Burlingame, CA). Tubules were combined and resuspended in medium that consisted of DMEM/F-12 culture media (Invitrogen) containing FCS (Life Technologies, 10%), insulin (Invitrogen, 5 μg/ml), transferrin (Sigma-Aldrich, St. Louis, MO; 5 μg/ml), selenite (Sigma-Aldrich, 5 ng/ml), dexamethasone (Sigma-Aldrich, 1 μmol/L), triiodothyronine (Sigma-Aldrich, 1 nmol/L), recombinant human EGF (Sigma-Aldrich, 0.01 mg/ml), and a 1% antibiotic/antimycotic solution (Sigma-Aldrich, 10,000 units/ml penicillin, 0.1 mg/ml streptomycin, and 0.25 mg/ml amphotericin B). Quality of isolated proximal tubules was confirmed by Western blot using rabbit megalin polyclonal antibody (a gift from Dr. T. Michigami).

Antibodies

We used the following antibodies: antibodies for guinea pig p62-specific (C-terminal–specific) polyclonal antibody (Progen, Heidelberg, Germany), mouse ubiquitin–specific monoclonal antibody (Cell Signaling Technology, Danvers, MA), mouse β-actin–specific monoclonal antibody (Sigma-Aldrich), Atg5-specific antibody (MBL, Tokyo, Japan), GFP-specific antibody (Roche, Mannheim, Germany), horseradish peroxidase–conjugated anti-rat antibody (DAKO, Glostrup, Denmark), biotinylated secondary antibodies (Vector Laboratories), and Alexa555- and Alexa488-conjugated secondary antibodies (Molecular Probes, Carlsbad, CA).

Biochemical Parameters

Serum urea nitrogen was measured using the Urea-nitrogen-Test-Wako (Wako). Urinary albumin, glucose, and inorganic phosphate were measured using the Albuwell M kit (Exocell, Philadelphia, PA), Glucose CII-Test-Wako (Wako), and intraperitoneally-HA-Test-Wako (Wako). Urinary amino acids were measured by capillary electrophoresis time-of-flight mass spectrometry as described previously.[48,49] Urinary markers were adjusted by urinary creatinine, which was measured using the CRE-EN Kainos (Kainos, Tokyo, Japan).

Western Blot Analysis

Isolated tissues were lysed in cell lysis buffer (Cell Signaling Technology) and a protease inhibitor cocktail, Complete Mini (Roche). Each sample was subject to immunoblot analysis as described previously.[50]

Statistical Analysis

All results are presented as means ± SD. Statistical significance among multiple experimental values was evaluated using ANOVA, followed by the Scheffe's procedure. The difference between two experimental values was assessed by a nonpaired *t* test. Statistical significance was defined as $P < 0.05$.

ACKNOWLEDGMENTS

We thank Noboru Mizushima, Tokyo Medical and Dental University, for the donation of the *Atg5*^{flox} mice and GFP-LC3 transgenic mice; Shinichi Uchida, Tokyo Medical and Dental University, for the plasmid containing mouse KAP genomic DNA; Jun-ichi Miyazaki, Osaka University, for the CAG-CAT-Z mice; Toshimi Michigami, Osaka Medical Center and Research Institute, for Maternal and Child Health, for the antibody to megalin; Yoshikatsu Kanai, Osaka University, for discussion; and Naoko Horimoto and Rica Harada for technical and secretary assistance. This research was supported by a Grant-in-Aid for Scientific Research from the Ministry of Education,

Culture, Sports, Science and Technology of Japan (22590890). Y.T., J.K., and Y.I. were supported by a grant from FLASH 2009 (PHarma-Link between Academia and Shionogi, J090701308).

DISCLOSURES

None.

REFERENCES

1. Mizushima N, Ohsumi Y, Yoshimori T: Autophagosome formation in mammalian cells. *Cell Struct Funct* 27: 421–429, 2002
2. Levine B, Klionsky DJ: Development by self-digestion: molecular mechanisms and biological functions of autophagy. *Dev Cell* 6: 463–477, 2004
3. Mizushima N, Levine B, Cuervo AM, Klionsky DJ: Autophagy fights disease through cellular self-digestion. *Nature* 451: 1069–1075, 2008
4. Levine B, Kroemer G: Autophagy in the pathogenesis of disease. *Cell* 132: 27–42, 2008
5. Hara T, Nakamura K, Matsui M, Yamamoto A, Nakahara Y, Suzuki-Migishima R, Yokoyama M, Mishima K, Saito I, Okano H, Mizushima N: Suppression of basal autophagy in neural cells causes neurodegenerative disease in mice. *Nature* 441: 885–889, 2006
6. Komatsu M, Waguri S, Ueno T, Iwata J, Murata S, Tanida I, Ezaki J, Mizushima N, Ohsumi Y, Uchiyama Y, Kominami E, Tanaka K, Chiba T: Impairment of starvation-induced and constitutive autophagy in Atg7-deficient mice. *J Cell Biol* 169: 425–434, 2005
7. Komatsu M, Waguri S, Chiba T, Murata S, Iwata J, Tanida I, Ueno T, Koike M, Uchiyama Y, Kominami E, Tanaka K: Loss of autophagy in the central nervous system causes neurodegeneration in mice. *Nature* 441: 880–884, 2006
8. Nakai A, Yamaguchi O, Takeda T, Higuchi Y, Hikoso S, Taniike M, Omiya S, Mizote I, Matsumura Y, Asahi M, Nishida K, Hori M, Mizushima N, Otsu K: The role of autophagy in cardiomyocytes in the basal state and in response to hemodynamic stress. *Nat Med* 13: 619–624, 2007
9. Mizushima N, Levine B: Autophagy in mammalian development and differentiation. *Nat Cell Biol* 12: 823–830, 2010
10. Epstein FH: Oxygen and renal metabolism. *Kidney Int* 51: 381–385, 1997
11. Torelli G, Milla E, Faelli A, Costantini S: Energy requirement for sodium reabsorption in the in vivo rabbit kidney. *Am J Physiol* 211: 576–580, 1966
12. Christensen EI, Nielsen S: Structural and functional features of protein handling in the kidney proximal tubule. *Semin Nephrol* 11: 414–439, 1991
13. Maack T, Johnson V, Kau ST, Figueiredo J, Sigulem D: Renal filtration, transport, and metabolism of low-molecular-weight proteins: A review. *Kidney Int* 16: 251–270, 1979
14. Suzuki C, Isaka Y, Takabatake Y, Tanaka H, Koike M, Shibata M, Uchiyama Y, Takahara S, Imai E: Participation of autophagy in renal ischemia/reperfusion injury. *Biochem Biophys Res Commun* 368: 100–106, 2008
15. Jiang M, Liu K, Luo J, Dong Z: Autophagy is a renoprotective mechanism during in vitro hypoxia and in vivo ischemia-reperfusion injury. *Am J Pathol* 176: 1181–1192, 2010
16. Periyasamy-Thandavan S, Jiang M, Wei Q, Smith R, Yin XM, Dong Z: Autophagy is cytoprotective during cisplatin injury of renal proximal tubular cells. *Kidney Int* 74: 631–640, 2008
17. Inoue K, Kuwana H, Shimamura Y, Ogata K, Taniguchi Y, Kagawa T, Horino T, Takao T, Morita T, Sasaki S, Mizushima N, Terada Y: Cisplatin-induced macroautophagy occurs prior to apoptosis in proximal tubules in vivo. *Clin Exp Nephrol* 14: 112–122, 2009
18. Sansanwal P, Yen B, Gahl WA, Ma Y, Ying L, Wong LJ, Sarwal MM: Mitochondrial autophagy promotes cellular injury in nephropathic cystinosis. *J Am Soc Nephrol* 21: 272–283, 2009
19. Pallet N, Bouvier N, Legendre C, Gilleron J, Codogno P, Beaune P, Thervet E, Anglicheau D: Autophagy protects renal tubular cells against cyclosporine toxicity. *Autophagy* 4: 783–791, 2008
20. Klionsky DJ, Abeliovich H, Agostinis P, Agrawal DK, Aliev G, Askew DS, Baba M, Baehrecke EH, Bahr BA, Ballabio A, Bamber BA, Bassham DC, Bergamini E, Bi X, Biard-Piechaczyk M, Blum JS, Bredesen DE, Brodsky JL, Brumell JH, Brunk UT, Bursch W, Camougrand N, Cebollero E, Cecconi F, Chen Y, Chin LS, Choi A, Chu CT, Chung J, Clarke PG, Clark RS, Clarke SG, Clave C, Cleveland JL, Codogno P, Colombo MI, Coto-Montes A, Cregg JM, Cuervo AM, Debnath J, Demarchi F, Dennis PB, Dennis PA, Deretic V, Devenish RJ, Di Sano F, Dice JF, Difiglia M, Dinesh-Kumar S, Distelhorst CW, Djavaheri-Mergny M, Dorsey FC, Droge W, Dron M, Dunn WA, Jr., Duszenko M, Eissa NT, Elazar Z, Esclatine A, Eskelinen EL, Fesus L, Finley KD, Fuentes JM, Fueyo J, Fujisaki K, Galliot B, Gao FB, Gewirtz DA, Gibson SB, Gohla A, Goldberg AL, Gonzalez R, Gonzalez-Estevez C, Gorski S, Gottlieb RA, Haussinger D, He YW, Heidenreich K, Hill JA, Hoyer-Hansen M, Hu X, Huang WP, Iwasaki A, Jaattela M, Jackson WT, Jiang X, Jin S, Johansen T, Jung JU, Kadowaki M, Kang C, Kelekar A, Kessel DH, Kiel JA, Kim HP, Kimchi A, Kinsella TJ, Kiselyov K, Kitamoto K, Knecht E, Komatsu M, Kominami E, Kondo S, Kovacs AL, Kroemer G, Kuan CY, Kumar R, Kundu M, Landry J, Laporte M, Le W, Lei HY, Lenardo MJ, Levine B, Lieberman A, Lim KL, Lin FC, Liou W, Liu LF, Lopez-Berestein G, Lopez-Otin C, Lu B, Macleod KF, Malorni W, Martinet W, Matsuoka K, Mautner J, Meijer AJ, Melendez A, Michels P, Miotto G, Mistiaen WP, Mizushima N, Mograbi B, Monastyrska I, Moore MN, Moreira PI, Moriyasu Y, Motyl T, Munz C, Murphy LO, Naqvi NI, Neufeld TP, Nishino I, Nixon RA, Noda T, Nurnberg B, Ogawa M, Oleinick NL, Olsen LJ, Ozpolat B, Paglin S, Palmer GE, Papassideri I, Parkes M, Perlmutter DH, Perry G, Piacentini M, Pinkas-Kramarski R, Prescott M, Proikas-Cezanne T, Raben N, Rami A, Reggiori F, Rohrer B, Rubinsztein DC, Ryan KM, Sadoshima J, Sakagami H, Sakai Y, Sandri M, Sasakawa C, Sass M, Schneider C, Seglen PO, Seleverstov O, Settleman J, Shacka JJ, Shapiro IM, Sibirny A, Silva-Zacarin EC, Simon HU, Simone C, Simonsen A, Smith MA, Spanel-Borowski K, Srinivas V, Steeves M, Stenmark H, Stromhaug PE, Subauste CS, Sugimoto S, Sulzer D, Suzuki T, Swanson MS, Tabas I, Takeshita F, Talbot NJ, Talloczy Z, Tanaka K, Tanida I, Taylor GS, Taylor JP, Terman A, Tettamanti G, Thompson CB, Thumm M, Tolkovsky AM, Tooze SA, Truant R, Tumanovska LV, Uchiyama Y, Ueno T, Uzcategui NL, van der Klei I, Vaquero EC, Vellai T, Vogel MW, Wang HG, Webster P, Wiley JW, Xi Z, Xiao G, Yahalom J, Yang JM, Yap G, Yin XM, Yoshimori T, Yu L, Yue Z, Yuzaki M, Zabirnyk O, Zheng X, Zhu X, Deter RL: Guidelines for the use and interpretation of assays for monitoring autophagy in higher eukaryotes. *Autophagy* 4: 151–175, 2008
21. Mizushima N, Yoshimori T, Levine B: Methods in mammalian autophagy research. *Cell* 140: 313–326, 2010
22. Ding Y, Davisson RL, Hardy DO, Zhu LJ, Merrill DC, Catterall JF, Sigmund CD: The kidney androgen-regulated protein promoter confers renal proximal tubule cell-specific and highly androgen-responsive expression on the human angiotensinogen gene in transgenic mice. *J Biol Chem* 272: 28142–28148, 1997
23. Kabeya Y, Mizushima N, Ueno T, Yamamoto A, Kirisako T, Noda T, Kominami E, Ohsumi Y, Yoshimori T: LC3, a mammalian homologue of yeast Apg8p, is localized in autophagosome membranes after processing. *EMBO J* 19: 5720–5728, 2000
24. Mizushima N, Yamamoto A, Matsui M, Yoshimori T, Ohsumi Y: In vivo analysis of autophagy in response to nutrient starvation using transgenic mice expressing a fluorescent autophagosome marker. *Mol Biol Cell* 15: 1101–1111, 2004
25. Bjorkoy G, Lamark T, Brech A, Outzen H, Perander M, Overvatn A,

Stenmark H, Johansen T: p62/SQSTM1 forms protein aggregates degraded by autophagy and has a protective effect on huntingtin-induced cell death. *J Cell Biol* 171: 603–614, 2005
26. Caro LH, Plomp PJ, Wolvetang EJ, Kerkhof C, Meijer AJ: 3-Methyladenine, an inhibitor of autophagy, has multiple effects on metabolism. *Eur J Biochem* 175: 325–329, 1988
27. Punnonen EL, Marjomaki VS, Reunanen H: 3-Methyladenine inhibits transport from late endosomes to lysosomes in cultured rat and mouse fibroblasts. *Eur J Cell Biol* 65: 14–25, 1994
28. Xue L, Borutaite V, Tolkovsky AM: Inhibition of mitochondrial permeability transition and release of cytochrome c by anti-apoptotic nucleoside analogues. *Biochem Pharmacol* 64: 441–449, 2002
29. Hosokawa N, Hara Y, Mizushima N: Generation of cell lines with tetracycline-regulated autophagy and a role for autophagy in controlling cell size. *FEBS Lett* 580: 2623–2629, 2006
30. Kuma A, Hatano M, Matsui M, Yamamoto A, Nakaya H, Yoshimori T, Ohsumi Y, Tokuhisa T, Mizushima N: The role of autophagy during the early neonatal starvation period. *Nature* 432: 1032–1036, 2004
31. Bagnasco S, Good D, Balaban R, Burg M: Lactate production in isolated segments of the rat nephron. *Am J Physiol* 248: F522–F526, 1985
32. Starkov AA: The role of mitochondria in reactive oxygen species metabolism and signaling. *Ann NY Acad Sci* 1147: 37–52, 2008
33. Balaban RS, Nemoto S, Finkel T: Mitochondria, oxidants, and aging. *Cell* 120: 483–495, 2005
34. Kim I, Rodriguez-Enriquez S, Lemasters JJ: Selective degradation of mitochondria by mitophagy. *Arch Biochem Biophys* 462: 245–253, 2007
35. Mizushima N: Autophagy: Process and function. *Genes Dev* 21: 2861–2873, 2007
36. Mizushima N, Yamamoto A, Hatano M, Kobayashi Y, Kabeya Y, Suzuki K, Tokuhisa T, Ohsumi Y, Yoshimori T: Dissection of autophagosome formation using Apg5-deficient mouse embryonic stem cells. *J Cell Biol* 152: 657–668, 2001
37. Hailey DW, Rambold AS, Satpute-Krishnan P, Mitra K, Sougrat R, Kim PK, Lippincott-Schwartz J: Mitochondria supply membranes for autophagosome biogenesis during starvation. *Cell* 141: 656–667, 2010
38. Vembar SS, Brodsky JL: One step at a time: Endoplasmic reticulum-associated degradation. *Nat Rev Mol Cell Biol* 9: 944–957, 2008
39. Schubert D, Behl C, Lesley R, Brack A, Dargusch R, Sagara Y, Kimura H: Amyloid peptides are toxic via a common oxidative mechanism. *Proc Natl Acad Sci USA* 92: 1989–1993, 1995
40. Relini A, Torrassa S, Rolandi R, Gliozzi A, Rosano C, Canale C, Bolognesi M, Plakoutsi G, Bucciantini M, Chiti F, Stefani M: Monitoring the process of HypF fibrillization and liposome permeabilization by protofibrils. *J Mol Biol* 338: 943–957, 2004
41. Lameire N, Van Biesen W, Vanholder R: Acute renal failure. *Lancet* 365: 417–430, 2005
42. Hochachka PW: Defense strategies against hypoxia and hypothermia. *Science* 231: 234–241, 1986
43. Brooks C, Wei Q, Cho SG, Dong Z: Regulation of mitochondrial dynamics in acute kidney injury in cell culture and rodent models. *J Clin Invest* 119: 1275–1285, 2009
44. Kraft C, Peter M, Hofmann K: Selective autophagy: Ubiquitin-mediated recognition and beyond. *Nat Cell Biol* 12: 836–841, 2010
45. Taniguchi M, Sanbo M, Watanabe S, Naruse I, Mishina M, Yagi T: Efficient production of Cre-mediated site-directed recombinants through the utilization of the puromycin resistance gene, pac: A transient gene-integration marker for ES cells. *Nucleic Acids Res* 26: 679–680, 1998
46. Asano T, Niimura F, Pastan I, Fogo AB, Ichikawa I, Matsusaka T: Permanent genetic tagging of podocytes: Fate of injured podocytes in a mouse model of glomerular sclerosis. *J Am Soc Nephrol* 16: 2257–2262, 2005
47. Sakai K, Miyazaki J: A transgenic mouse line that retains Cre recombinase activity in mature oocytes irrespective of the cre transgene transmission. *Biochem Biophys Res Commun* 237: 318–324, 1997
48. Soga T, Ishikawa T, Igarashi S, Sugawara K, Kakazu Y, Tomita M: Analysis of nucleotides by pressure-assisted capillary electrophoresis-mass spectrometry using silanol mask technique. *J Chromatogr A* 1159: 125–133, 2007
49. Soga T, Baran R, Suematsu M, Ueno Y, Ikeda S, Sakurakawa T, Kakazu Y, Ishikawa T, Robert M, Nishioka T, Tomita M: Differential metabolomics reveals ophthalmic acid as an oxidative stress biomarker indicating hepatic glutathione consumption. *J Biol Chem* 281: 16768–16776, 2006
50. Matsui I, Hamano T, Mikami S, Fujii N, Takabatake Y, Nagasawa Y, Kawada N, Ito T, Rakugi H, Imai E, Isaka Y: Fully phosphorylated fetuin-A forms a mineral complex in the serum of rats with adenine-induced renal failure. *Kidney Int* 75: 915–928, 2009

Supplemental information for this article is available online at http://www.jasn.org/.